

# Movement of mitral fibrous components in an isolated porcine working heart model

Akinori Tamenishi, Yoshimori Araki, Shunei Saito, Hideki Oshima, Yuichi Ueda and Akihiko Usui

## Abstract

**Background:** There is little research regarding the movement of mitral fibrous components. We analyzed changes in mitral fibrous components in normal and deteriorated isolated working swine hearts.

**Methods:** In 5 swine hearts, 6 sonomicrometry transducers were placed around the mitral annulus and 2 in the papillary muscle tip. During the working cycle, we evaluated the annular dimension and calculated the contraction range and contraction ratio during the cardiac cycle in normal and deteriorated modes.

**Results:** The transverse ( $24.5 \pm 2.3$  vs.  $27.4 \pm 2.4$  mm) and posterior longitudinal diameter ( $18.3 \pm 7.0$  vs.  $22.5 \pm 5.5$  mm) increased significantly in deteriorated mode. The contraction range in transverse ( $1.8 \pm 0.6$  vs.  $0.8 \pm 0.7$  mm) and posterior longitudinal ( $1.6 \pm 0.6$  vs.  $0.8 \pm 0.3$  mm) diameters decreased significantly in deteriorated mode. The contraction range of the strut chordae was less than 1.0 mm in both modes, with no significant differences. The contraction ratio of the anterior strut chordae was significantly reduced in deteriorated mode ( $3.2 \pm 1.1\%$  vs.  $2.2 \pm 1.1\%$ ). The contraction ratio of the annulus was significantly lower in deteriorated mode with respect to transverse ( $6.9 \pm 2.1\%$  vs.  $2.9 \pm 2.9\%$ ) and longitudinal ( $13.3 \pm 4.5\%$  vs.  $8.6 \pm 5.1\%$ ) diameters.

**Conclusions:** In the deteriorated hearts, the mitral annulus was dilated and contractility decreased. The length of the strut chordae differed 1 mm between the deteriorated and normal modes; however, the contraction ratio of the anterior chordae during the cardiac cycle was reduced, indicating increased stretching.

## Keywords

Biomechanical phenomena, Heart ventricles, Mitral valve, Papillary muscles, Ventricular function, Swine

## Introduction

The structure and function of the mitral valve are physiologically complex. The mitral valve comprises leaflets, annulus, chordae, and papillary muscles. All mitral components work closely together during the cardiac cycle. These structures, except for the papillary muscles, are composed of fibrous components that possess less motility than muscle components. Previous studies have shown that the mitral annulus which consists of fibrous tissue, exhibits contractile activity, although the extent of contractility remains unclear.<sup>1–4</sup> In this study, we investigated the movement of fibrous components of the mitral valve during the cardiac cycle between systole and diastole under normal cardiac function (normal mode) and deteriorated

cardiac function (deteriorated mode) in the same heart, using an animal model.

## Materials and methods

The Nagoya University Laboratory Research Animal Care and Ethics Committee approved the research protocol. The investigation conformed to the

---

Department of Cardiac Surgery, Nagoya University Graduate School of Medicine, Nagoya, Japan

### Corresponding author:

Yoshimori Araki, Department of Cardiac Surgery, Nagoya University Graduate School of Medicine, 65 Tsurumai-cho, Showa-ku, Nagoya, Aichi 466-8550, Japan.

Email: yaraki@med.nagoya-u.ac.jp

Principles of Laboratory Animal Care formulated by the National Society for Medical Research and the Guide for the Care and Use of Laboratory Animals published by the National Institutes of Health, as revised in 1996. Five Landrace and Yorkshire pigs weighing 40–45 kg were used in this study. The animals were anesthetized with intramuscular ketamine  $7.5 \text{ mg kg}^{-1}$ , intubated with a 5.5-mm tube, and mechanically ventilated after tracheotomy. Anesthesia was maintained by inhalation of 0.02%–0.04% halothane. The heart was exposed via a median sternotomy. Following crossclamping of the descending aorta, 500 mL of cold St. Thomas' Hospital no. 2 solution (Miotecter, Kobayashi Pharmaceutical, Osaka, Japan) was infused into the coronary arteries via the right carotid artery. After complete cardiac arrest was confirmed, the heart and lungs were extracted en bloc.

The sonomicrometry system (10 MHz; Sonometrics, London, ON, Canada) is an instrument used to measure the distance between transducer crystals by means of ultrasound. The crystals are 2-mm diameter probes with electrical wires connected to the sonomicrometry device. The distance between each crystal can be measured simultaneously. Six crystals were placed in the mitral annulus via a left atrial incision, and 2 crystals were placed in the anterior and posterior papillary muscles via the left ventricular (LV) apex, as shown in Figure 1: Two crystals were positioned in the anterior

papillary muscle tip (1) and the posterior papillary muscle tip (2). The mitral annular dimension was measured by 6 crystals positioned at the anterior trigone (3), the posterior trigone (4), the right side of the annulus (5), the base of each posterior lateral right (6) and left (7) scallop, and the left side of the annulus (8). The distance between the right and left sides of the annulus (points 5 and 8) is the transverse diameter. After the crystals were positioned, the left atrium was closed. The lung lobes were bound tightly at the pulmonary hilum to separate the connections between the lung vessels and the left atrial chamber. The isolated heart was connected to a working heart apparatus, and perfusion was resumed in Langendorff mode.

The details of the working heart apparatus have been described in our previous reports.<sup>5,6</sup> The apparatus is designed to perfuse the isolated heart in either working heart mode or Langendorff mode, as shown in Figure 2. The crystalloid perfusate consisted of modified Krebs-Ringer solution: NaCl  $120.0 \text{ mmol L}^{-1}$ ; KCl  $4.0 \text{ mmol L}^{-1}$ ;  $\text{MgSO}_4 \cdot 7\text{H}_2\text{O}$   $1.3 \text{ mmol L}^{-1}$ ;  $\text{NaH}_2\text{PO}_4 \cdot 2\text{H}_2\text{O}$   $1.2 \text{ mmol L}^{-1}$ ;  $\text{CaCl}_2 \cdot 2\text{H}_2\text{O}$   $1.2 \text{ mmol L}^{-1}$ ;  $\text{NaHCO}_3$   $25.2 \text{ mmol L}^{-1}$ ; and glucose  $11.0 \text{ mmol L}^{-1}$ . Oxygenation was achieved with dissolved oxygen. The afterload was set 100 cm higher than the heart, and the preload was controlled by moving the preload column up and down. In this model, the isolated heart continued to work for 180 min while keeping ventricular

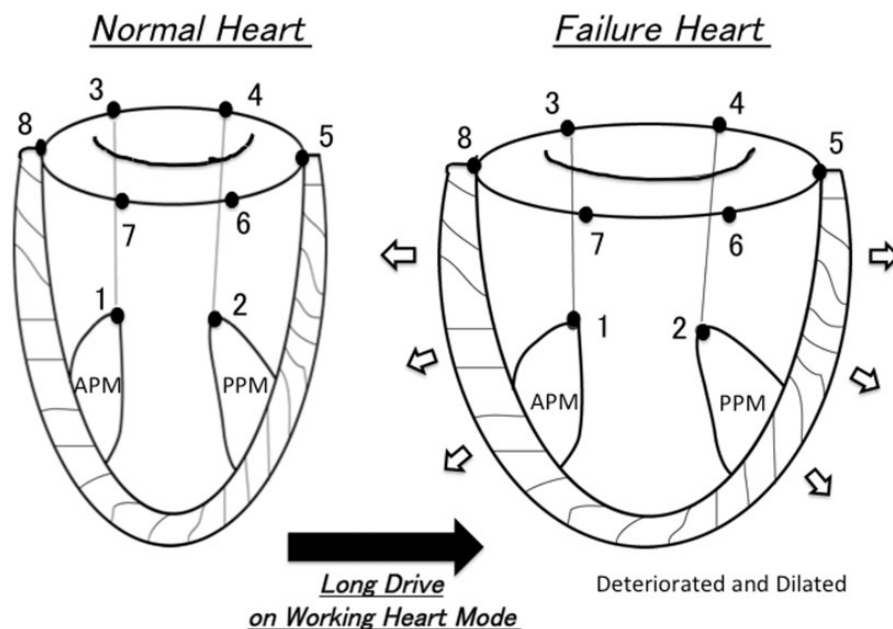


**Figure 1.** Schema of this study concept and location of the sonomicrometry tips. Two crystals were positioned in the anterior papillary muscle tip (1) and posterior papillary muscle tip (2). The mitral annular dimension was divided by 6 crystals positioned at the anterior trigone (3), the posterior trigone (4), the right side of the annulus (5), the base of each posterior lateral right (6) and left (7) scallops, and the left side of the annulus (8). The distance between points 5 and 8 is the transverse diameter. APM: anterior papillary muscle; PPM: posterior papillary muscle.

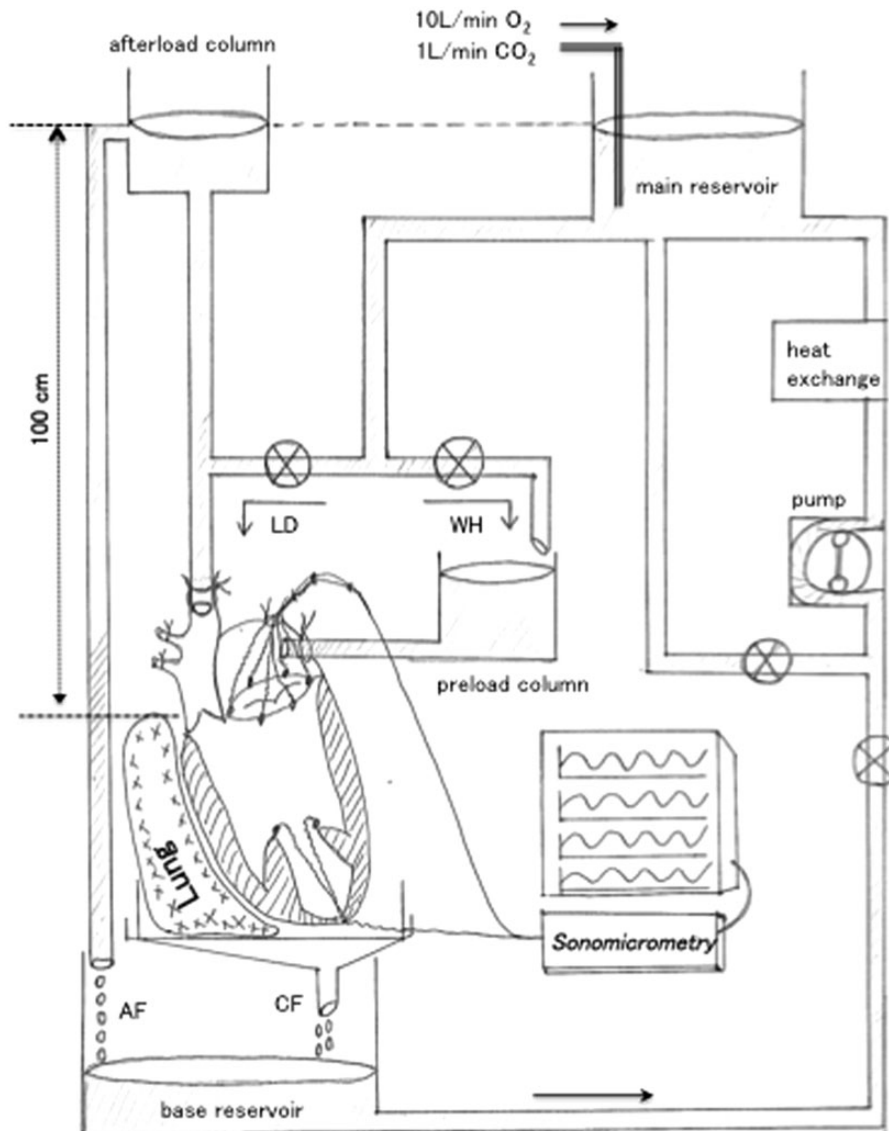


**Figure 2.** The isolated working heart apparatus. AF: aortic flow; CF: coronary flow; LD: Langendorff mode; WH: working heart mode.

function constant; however, after 180 min, ventricular function became gradually impaired, and finally deteriorated at 240 min.<sup>5</sup> When ventricular function deteriorates, the systemic pressure decreases and the preload must be increased by lifting the preload column to maintain the afterload. For pressure studies, a 5F micromanometer-tipped catheter (MPC-500; Millar Instruments, Houston, TX, USA) was introduced into the mid-position of the LV via the apex, and another catheter was introduced into the left atrium via the left atrial appendage. Epicardial electrodes were applied to obtain electrocardiograms. The data were recorded using our multiple-acquisition system (Leg-1000; Nihon Kohden, Tokyo, Japan; and Dipp-Motion 2D; Ditect, Tokyo, Japan). In this system, the LV pressure was differentiated simultaneously with respect to time,

and the real-time  $dP/dt$  of the LV was obtained. Normal LV function was defined as  $dP/dt > 800$  mm Hg/s, and deteriorated ventricular function was defined as  $dP/dt < 400$  mm Hg/s. After the beating of the heart had stabilized, the perfusion system was changed to working heart mode. Real-time sonomicrometry data were recorded in normal and deteriorated mode as LV function became impaired. The data exhibited a wave pattern during the cardiac cycle, allowing detection of the maximum and minimum values. Each parameter was evaluated during motion of the structure, and each motion during the cardiac cycle was analyzed for median length, contraction range, and contraction ratio, as follows: median length = (maximum distance + minimum distance)/2; contraction range = maximum distance - minimum distance

(mm); contraction ratio = contraction range/maximum distance  $\times$  100%. The median distance, contraction range, and contraction ratio in normal and deteriorated modes were compared.

All data are summarized as mean  $\pm$  standard deviation. Differences between 2 groups were analyzed using the paired *t* test. A *p* value less than 0.05 was considered statistically significant.

## Results

The hemodynamic characteristics of all 5 hearts are summarized in Table 1. In the deteriorated hearts, LV pressure gradually decreased, thus to maintain ventricular pressure, the left atrial pressure had to be increased by lifting the preload column. The median length of each distance is shown in Table 2. The lengths of all distances in the deteriorated heart, except the distance between papillary muscles, increased significantly compared to those observed in normal mode. However, the anterior-posterior papillary muscle distance showed a tendency for increased median length in deteriorated mode. The transverse annulus diameter, expressed by the distance between points 5 and 8, was significantly increased (by  $3.0 \pm 0.6$  mm) in deteriorated mode compared to normal mode ( $p < 0.05$ ). The posterior longitudinal annulus diameter (distance between points 4 and 6) was also significantly increased (by  $4.2 \pm 2.4$  mm) in deteriorated mode ( $p < 0.01$ ). The contraction range of each distance is shown in Table 3. There were no significant differences between the normal and deteriorated modes regarding the contraction range of the papillary muscles (1–2), anterior strut chordae (1–3), and posterior strut chordae (2–4). Regarding the transverse diameter, the range was  $1.8 \pm 0.6$  mm in normal mode and  $0.8 \pm 0.7$  mm in deteriorated mode ( $p < 0.05$ ). Regarding the longitudinal diameter of the posterior side (between points 4 and 6), the range was  $1.6 \pm 0.6$  mm in normal mode and  $0.8 \pm 0.3$  mm in deteriorated mode ( $p < 0.05$ ). The contraction ratio of each distance is shown in Table 4. Although the contraction ratio of the posterior strut chordae did not show a significant difference ( $2.4\% \pm 1.4\%$  in normal mode vs.  $1.8\% \pm 0.8\%$  in

deteriorated mode), a tendency to decrease was observed. The contraction ratio of the longitudinal and transverse annulus diameters differed significantly ( $p < 0.05$ ) between normal and deteriorated modes.

**Table 2.** The median length of each mitral distance in normal and deteriorated modes.

Position no.	Normal (mm)	Deteriorated (mm)	Difference	<i>p</i> value
<b>APM-PPM</b>				
1–2	16.7 $\pm$ 3.1	18.3 $\pm$ 3.7	1.6 $\pm$ 1.3	0.051
<b>Anterior chordae</b>				
1–3	22.5 $\pm$ 1.1	23.7 $\pm$ 0.9	1.3 $\pm$ 0.3	<0.001
1–8	21.1 $\pm$ 4.1	22.1 $\pm$ 4.4	1.1 $\pm$ 0.4	<0.01
1–7	18.5 $\pm$ 3.2	19.2 $\pm$ 3.2	0.6 $\pm$ 0.5	<0.05
<b>Posterior chordae</b>				
2–4	27.2 $\pm$ 1.4	28.1 $\pm$ 1.5	0.8 $\pm$ 0.2	<0.001
2–5	22.4 $\pm$ 3.2	22.9 $\pm$ 3.1	0.5 $\pm$ 0.4	<0.05
2–6	25.1 $\pm$ 3.3	26.6 $\pm$ 3.7	1.5 $\pm$ 0.4	<0.001
<b>Annulus diameter</b>				
5–8	24.5 $\pm$ 2.3	27.4 $\pm$ 2.4	3.0 $\pm$ 0.6	<0.001
3–7	14.6 $\pm$ 4.3	16.2 $\pm$ 4.9	1.6 $\pm$ 1.4	<0.05
4–6	18.3 $\pm$ 7.0	22.5 $\pm$ 5.5	4.2 $\pm$ 2.4	<0.01

Position 5–8 of the annulus diameter shows the transverse diameter, position 4–6 of the annulus diameter shows the posterior longitudinal diameter. APM: anterior papillary muscle; PPM: posterior papillary muscle.

**Table 3.** Contraction range of each mitral distance during the cardiac cycle in normal and deteriorated modes.

Position no.	Normal (mm)	Deteriorated (mm)	<i>p</i> value
<b>APM-PPM</b>			
1–2	2.7 $\pm$ 1.2	2.4 $\pm$ 1.1	0.404
<b>Anterior chordae</b>			
1–3	0.7 $\pm$ 0.2	0.5 $\pm$ 0.2	0.052
1–8	0.8 $\pm$ 0.4	0.5 $\pm$ 0.6	<0.05
1–7	0.8 $\pm$ 0.3	0.5 $\pm$ 0.5	<0.05
<b>Posterior chordae</b>			
2–4	0.7 $\pm$ 0.4	0.5 $\pm$ 0.2	0.168
2–5	1.1 $\pm$ 0.7	0.7 $\pm$ 0.3	0.115
2–6	1.2 $\pm$ 0.5	0.7 $\pm$ 0.3	0.072
<b>Annulus diameter</b>			
5–8	1.8 $\pm$ 0.6	0.8 $\pm$ 0.7	<0.05
3–7	2.1 $\pm$ 0.7	1.5 $\pm$ 0.9	0.055
4–6	1.6 $\pm$ 0.6	0.8 $\pm$ 0.3	<0.05

Position 1–3 of the anterior chorda shows the anterior strut chorda. Position 2–4 of the posterior chordae shows the posterior strut chorda. APM: anterior papillary muscle; PPM: posterior papillary muscle.

**Table 1.** Hemodynamic characteristics of the working heart model during normal and deteriorated function.

Parameter	Normal	Deteriorated	<i>p</i> value
Left ventricular pressure (mm Hg)	111.8 $\pm$ 4.9	73.6 $\pm$ 3.3	<0.001
Left atrial pressure (mm Hg)	10.2 $\pm$ 2.2	24.0 $\pm$ 2.9	<0.001
dP/dt (mm Hg/s)	815.8 $\pm$ 11.3	380.0 $\pm$ 8.9	<0.001

**Table 4.** Contraction ratio of each mitral distance in normal and deteriorated modes.

Position no.	Normal (mm)	Deteriorated (mm)	p value
<b>APM-PPM</b>			
1-2	15.3% ± 8.0%	13.0% ± 6.0%	0.331
<b>Anterior chordae</b>			
1-3	3.2% ± 1.1%	2.2% ± 1.1%	<0.05
1-8	3.6% ± 1.8%	2.2% ± 1.5%	<0.05
1-7	4.4% ± 1.8%	2.7% ± 2.7%	<0.05
<b>Posterior chordae</b>			
2-4	2.4% ± 1.4%	1.8% ± 0.8%	0.074
2-5	4.5% ± 2.4%	2.7% ± 1.0%	0.108
2-6	4.3% ± 1.4%	2.7% ± 1.3%	0.063
<b>Annulus diameter</b>			
5-8	6.9% ± 0.6%	2.9% ± 2.9%	<0.05
3-7	13.4% ± 4.5%	8.6% ± 5.1%	<0.05
4-6	9.1% ± 4.5%	3.8% ± 2.1%	<0.05

APM: anterior papillary muscle; PPM: posterior papillary muscle.

## Discussion

Many experimental models of mitral valve function have been described,<sup>7-9</sup> as have many procedures regarding the heart failure model. Nonetheless, it is difficult to create a model that suitably represents the clinical situation. The heart failure model used in this study was an acute rather than chronic failure model. Furthermore, it was not a localized ischemic model but a global deterioration model. It is well known that acute heart failure differs markedly from chronic heart failure in that acute heart failure does not involve the process of remodeling. However, we considered that the tendency for geometric remodeling would be the same when the contraction of the LV deteriorates during lengthy perfusion of crystalloid perfusate and when the chamber is filled with a significant preload. The advantage of this study protocol is that it allows comparisons in the same heart between normal and deteriorated function. In the deteriorated heart, the chamber expands and contractility weakens. However, the changes in geometry that occur when the ventricle is expanded have not yet been elucidated. In particular, the relationship between the mitral annulus and the mitral apparatus in the dilated heart is unclear. The strut chordae, anterior leaflet, bilateral trigone, and anterior annulus consist of fibrous tissue and seem to construct an arch, as shown in an intracardiac image taken with a high-speed camera, reported by us previously.<sup>6</sup> We had a strong interest in how this arch of fibrous tissue changes when the chamber is expanded.

This study established two important points, the first being the ratio of annular movement which contracts in the systolic phase. The other is that there is a difference in the contraction ratio of the second chordae between normal and deteriorated hearts, which is considered to be of fixed length during the cardiac cycle. Regarding the former point, in general, the mitral annulus consists of fibrous tissue; therefore, it does not have the ability to actively contract. However, annular contraction has been proved in many reports. There are few reports demonstrating the inherent value of the contraction ratio of the mitral annulus. This is most likely due to difficulties in adhering closely to anatomic points on the annulus using traditional or 3-dimensional echocardiography in clinical studies.<sup>10</sup> In studies on animal models, markers must be placed on the mitral annulus during cardiac arrest, which requires careful manipulation. Many reports have described the dynamics of the annulus, but few have proposed the value of the contraction ratio. The Stanford group studied annular motion using a radiopaque marker.<sup>11</sup> The contraction ratio was not calculated, although it was most likely almost 10% when calculated as 27.7 mm in diastole and 25.9 mm in systole. This result is almost compatible with our data of 6.9%–13.4%. In the deteriorated heart, we demonstrated that the mitral annulus was dilated and the contraction ratio of the annulus was significantly reduced to 2.9%–8.6%. These results raise the clinical issue of annuloplasty ring selection; whereas a flexible ring should be applied in a normally functioning heart to maintain annulus contractility, a rigid ring may be a better option in a failing heart because the annulus is out of action.

With respect to the latter point, the strut chordae maintain extension during the cardiac cycle and do not become slack in the diastolic phase, unlike other chordae. This fact was proved in our previous report in which strut chordae movement was observed with a high-speed camera, and in other reports of animal experiments.<sup>12,13</sup> However, the results of the present study indicate that the strut chordae do not loosen, although they do extend to a slight degree in synchronization with the cardiac cycle. In the normal heart, we found that the contraction ratio of the strut chordae was 2.4%–3.2%, whereas it was 1.8%–2.2% in the deteriorated heart. This indicates that the strut chordae of the deteriorated heart are more stretched than those of the normal heart, and the papillary muscle creates traction with the strut chordae due to expansion of the LV chamber. This logic is involved in the mechanism of tethering. Therefore, in terms of clinical application, this study helps to elucidate the mechanism of mitral tethering. In addition, analysis of the contraction ratio of the mitral annulus in normal and deteriorated



function will help in selecting the appropriate type of prosthetic ring.

This study had some limitations. It was designed as a porcine working heart model, which does not fully resemble the human heart in a living body. The annular shape was not analyzed as a 3-dimensional saddle shape, but an analysis of the distance between two points using crystals was performed. A 3-dimensional construction can be made only by gathering two-point distances. Therefore, we consider that the foundation of a 3-dimensional analysis is a 2-dimensional analysis. We did not estimate the degree of mitral regurgitation, which is a key issue regarding heart failure and surgical intervention in clinical practice. Thus the assessment of mitral regurgitation while function is deteriorating might be important. Further studies are expected to elucidate the mechanism of the relationship between mitral regurgitation and deteriorating cardiac function.

We concluded that the mitral apparatus was stretched and mobility was significantly decreased in the deteriorated mode compared to normal function. The contraction ratio of the mitral annulus diameter during normal function was 6.9%–13.4%, however, that of the deteriorated heart was reduced to 2.9%–8.6%, and the mitral annulus itself was significantly dilated. The decreased contraction ratio of the strut chordae observed in the deteriorated mode indicates increasing traction from the papillary muscles as a result of ventricular expansion.

### Acknowledgments

The authors gratefully acknowledge Professor Nobuyuki Hamajima of Nagoya University Graduate School of Medicine for his valuable advice on the statistical analysis, and Akira Oonishi of the Gene Research Center, University of Tsukuba, for supplying the animals used in this study.

### Funding

This research received no specific grant from any funding agency in the public, commercial, or not-for-profit sectors.

### Conflict of interest statement

None declared.

### References

- Grewal J, Suri R, Mankad S, et al. Mitral annular dynamics in myxomatous valve disease: new insights with real-time 3-dimensional echocardiography. *Circulation* 2010; 121: 1423–1431.
- Itoh A, Ennis DB, Bothe W, et al. Mitral annular hinge motion contribution to changes in mitral septal-lateral dimension and annular area. *J Thorac Cardiovasc Surg* 2009; 138: 1090–1099.
- Stevanella M, Votta E and Redaelli A. Mitral valve finite element modeling: implications of tissues' nonlinear response and annular motion. *J Biomech Eng* 2009; 131: 121010.
- Jensen H, Jensen MO, Ringgaard S, et al. Geometric determinants of chronic functional ischemic mitral regurgitation: insights from three-dimensional cardiac magnetic resonance imaging. *J Heart Valve Dis* 2008; 17: 16–22.
- Araki Y, Usui A, Kawaguchi O, et al. Pressure-volume relationship in isolated working heart with crystalloid perfusate in swine and imaging the valve motion. *Eur J Cardiothorac Surg* 2005; 28: 435–442.
- Saito S, Araki Y, Usui A, et al. Mitral valve motion assessed by high-speed video camera in isolated swine heart. *Eur J Cardiothorac Surg* 2006; 30: 584–591.
- Opdahl A, Remme EW, Helle-Valle T, et al. Determinants of left ventricular early-diastolic lengthening velocity: independent contributions from left ventricular relaxation, restoring forces, and lengthening load. *Circulation* 2009; 119: 2578–2586.
- Parish LM, Jackson BM, Enomoto Y, Gorman RC and Gorman JH 3rd. The dynamic anterior mitral annulus. *Ann Thorac Surg* 2004; 78: 1248–1255.
- Gorman JH 3rd, Jackson BM, Enomoto Y and Gorman RC. The effect of regional ischemia on mitral valve annular saddle shape. *Ann Thorac Surg* 2004; 77: 544–548.
- Foster GP, Dunn AK, Abraham S, Ahmadi N and Sarraf G. Accurate measurement of mitral annular dimensions by echocardiography: importance of correctly aligned imaging planes and anatomic landmarks. *J Am Soc Echocardiogr* 2009; 22: 458–463.
- Dagum P, Timek T, Green GR, et al. Three-dimensional geometric comparison of partial and complete flexible mitral annuloplasty rings. *J Thorac Cardiovasc Surg* 2001; 122: 665–673.
- Nonaka M, Marui A, Fukuoka M, et al. Differences in mitral valve-left ventricle dimensions between a beating heart and during saline injection test. *Eur J Cardiothorac Surg* 2008; 34: 755–759.
- Joudinaud TM, Kegel CL, Flecher EM, et al. The papillary muscles as shock absorbers of the mitral valve complex. An experimental study. *Eur J Cardiothorac Surg* 2007; 32: 96–101.